Available online at www.sciencedirect.com
ScienceDirect
Developmental Biology 315 (2008) 99–113
DEVELOPMENTAL BIOLOGY
www.elsevier.com/developmentalbiology

Ordered progression of nematogenesis from stem cells through differentiation stages in the tentacle bulb of *Clytia hemisphaerica* (Hydrozoa, Cnidaria)

Elsa Denker*, Michaël Manuel, Lucas Leclère, Hervé Le Guyader, Nicolas Rabet

Université Pierre et Marie Curie-Paris 6, UMR 7138 CNRS UPMC MNHN IRD, Case 05, 7 quai St. Bernard, 75005 Paris, France

Received for publication 9 November 2007; revised 11 December 2007; accepted 11 December 2007
Available online 27 December 2007

Abstract

Nematogenesis, the production of stinging cells (nematocytes) in Cnidaria, can be considered as a model neurogenic process. Most molecular data concern the freshwater polyp *Hydra*, in which nematocyte production is scattered throughout the body column ectoderm, the mature cells then migrating to the tentacles. We have characterized tentacular nematogenesis in the *Clytia hemisphaerica* hydromedusa and found it to be confined to the ectoderm of the tentacle bulb, a specialized swelling at the tentacle base. Analysis by a variety of light and electron microscope techniques revealed that while cellular aspects of nematogenesis are similar to *Hydra*, the spatio-temporal characteristics are markedly more ordered. The tentacle bulb nematogenic ectoderm (TBE) was found to be polarized, with a clear progression of successive nematoblast stages from a proximal zone (comprising a majority of undifferentiated cells) to the distal end where the tentacle starts. Pulse-chase labelling experiments demonstrated a continuous displacement of differentiating nematoblasts towards the tentacle tip, and that nematogenesis proceeds more rapidly in *Clytia* than in *Hydra*. Compact expression domains of orthologues of known nematogenesis-associated genes (*Piwi*, *dickkopf-3*, *minicollagens* and *NOWA*) were correspondingly staggered along the TBE. These distinct characteristics make the *Clytia* TBE a promising experimental system for understanding the mechanisms regulating nematogenesis.

Keywords: Cnidaria; *Clytia hemisphaerica*; Nematocyte; Nematogenesis; Medusa; Tentacle bulb; *Minicollagens*; *Piwi*; *NOWA*; *Dickkopf-3*

Introduction

The Cnidaria (jellyfishes, corals, anemones, hydras, etc.) is a highly diversified and successful animal phylum, exhibiting a large variety of habitats, morphologies and life cycles (Brusca and Brusca, 2003; Collins et al., 2006); however, all cnidarians share a common highly specialized and unique cell type, the nematocyte. These single use stinging cells fulfill a predatory, defensive and sometimes locomotive role (Kass-Simon and Scappaticci, 2002). They occur at a particularly high concentration on the tentacles and mouth. Nematocyte discharge results from stimulation of the cnidocil ciliary cone apparatus by external mechanical and chemosensory stimuli, in some cases facilitated by signals coming from neighbouring cells through afferent synapses. The discharge process involves exocytosis of a complex organelle, the nematocyst, and explosive devagination of a poison-injecting thread, which prior to discharge is kept coiled under pressure within the nematocyst wall (Holstein and Tardent, 1984; Nüchter et al., 2006; Thurm et al., 2004).

Nematogenesis, the multistep process of nematocyte production, is a particularly interesting process from developmental and evolutionary points of view because nematocytes are thought to be highly derived neuro-sensory cells (Hausmann and Holstein, 1985; Brinkmann et al., 1996; Westfall, 1996; Miljkovic-Licina et al., 2004). Nematocytes and typical neurosensory cells share the ability to detect and integrate sensory and neuronal stimuli and to transmit efferent action potentials (Thurm et al., 2004). In hydrozoans, they are also produced from the same stem cell lineage (the interstitial stem cell system) (Lentz, 1966; Burnett, 1968; David and Gierer, 1974; David and Murphy, 1977). Finally, the production, integration and innervation of fully functional nematocytes from early nematoblasts committed among stem cells is likely to involve numerous regulator and effector genes, and among them bilaterian neural gene homologues were found to be

* Corresponding author. Fax: +33 1 44 27 58 01.
E-mail address: elsa.denker@snv.jussieu.fr (E. Denker).

0012-1606/$ - see front matter © 2007 Elsevier Inc. All rights reserved.
doi:10.1016/j.ydbio.2007.12.023

expressed during nematogenesis (such as the cnidarian achaete-scute homologue *CnASH* (Grens et al., 1995; Lindgens et al., 2004; Müller et al., 2003), the cnidarian *Zic* gene (Lindgens et al., 2004), the *paired*-like gene *prdl-b* and *COUP-TF* genes (Gauchat et al., 2004; Miljkovic-Licina et al., 2004). Understanding nematogenesis can thus provide insights about fundamental neurogenesis processes in the common Cnidaria/Bilateria ancestor.

In *Hydra*, interstitial stem cells are continuously committed to a nematoblast fate at multiple sites scattered throughout the ectoderm of the body column, excluding the pedal and oral parts of the polyp (David and Challoner, 1974; David and Gierer, 1974). The interstitial cell population, which occupy a position between the myoepithelial cells, comprises multipotent stem cells as well as their derivatives: the committed precursors, differentiating intermediates and mature forms of neurons, nematocytes, glandular cells and germ cells (Bode and David, 1978; David and Murphy, 1977; Bode 1996). Recently, the existence of an intermediate bipotent stem cell giving rise to both nematocytes and neurons (ganglion cells), expressing the *Cnox2* homeobox gene, has been reported (Miljkovic-Licina et al., 2007).

The various steps of nematocyte differentiation in *Hydra* have been described by Slautterback and Fawcett (1959) and Holstein (1981) (see also Bode, 1988). Early committed nematoblasts undergo a change in nuclear morphology, and after an initial division, they remain interstitial and divide synchronously as a syncitial cell cluster of 4 to 32 cells. Terminal differentiation can occur after any of these division steps. Cells undergo a first growth phase, during which the nematocyst primordium forms as a Golgi-derived organelle. This occurs just before the terminal division that marks the beginning of the second growth phase. Then the tubule, a distinct structure that gives rise to the harpoon thread, develops within the cytoplasm through the fusion of vesicles. When this stage is completed, the tubule invaginates into the capsule. The capsule maturates and the tubule differentiates into a shaft and a thread covered with spines. The cnidocil apparatus forms, and the capsule wall becomes thinner and acquires its high tensile strength. The final maturation step involves the synthesis of poly-γ-glutamate within the nematocyst wall, responsible for generating the huge internal pressure that will allow discharge (Szczepanek et al., 2002). At this point, the cluster splits into individual mature nematocytes that migrate towards the tentacle to be inserted into the nematocyte batteries in association with support cells.

Our current knowledge of the nematogenesis process derives mainly from extensive studies in the freshwater hydrozoan *Hydra*. *Hydra* has proved to be a powerful experimental model to investigate morphogenetic processes involved in adult tissue homeostasis and regeneration (Galliot and Schmid, 2002), but it lacks the medusa stage present in the ancestral life cycle of *Hydrozoa*. The medusae of hydrozoan species such as *Clytia* and *Podocoryne* have a distinct nervous and muscular organization compared to the polyp stages, reflecting different lifestyles and behaviors (Brusca and Brusca, 2003). The study of a variety of species and life-cycle stages will aid the identification of conserved and derived developmental mechanisms. In particular, the evolutionary significance of nematogenesis as a model of non-bilaterian neurogenesis will emerge only when cnidarian ancestral features can be sorted from lineage specific apomorphic features.

We have studied nematogenesis in medusae of the leptothecate hydrozoan *Clytia hemisphaerica* (Linnaeus, 1767), which has recently been developed as a model species for developmental studies (Chevalier et al., 2006; Momose and Houliston, 2007). The *Clytia* medusa is relatively large (about 1 cm diameter), transparent and lives for 2 to 3 months. Histological studies have shown that nematogenesis in hydrozoan medusae occurs in specialized zones separate from the final destination of the mature nematocytes. Oral nematocytes are produced at the base of the manubrium (the structure that bears the mouth) and tentacle nematocytes in the tentacle bulbs: spherical outgrowths on the bell margin from which tentacles grow (Bouillon, 1994). Newly hatched *Clytia* medusae have 4 tentacle bulbs and adults about 24, new bulbs being inserted during medusa growth.

Here we present the tentacle bulb of the *C. hemisphaerica* (Hydrozoa) medusa as a novel model to study nematogenesis. We have characterized the sequence of nematogenesis by a variety of techniques of light and electron microscopy, including histological staining and fluorescent labelling; we then monitored cell division and nematocyst migration and performed *in situ* hybridization of selected markers of nematogenesis stages. We show that the general cytological and molecular aspects of nematocyte differentiation are similar to *Hydra*, but with a very distinct, highly ordered spatio-temporal organization. Not only is nematogenesis confined to a specialized structure, but it involves a spatio-temporal progression of nematogenesis stages along the proximo-distal axis of the bulb. Such properties open perspectives for future experimental studies of nematogenesis using *Clytia*.

Materials and methods

Animal cultures

For all experiments, we used *C. hemisphaerica* medusae cultured in our lab in Paris. Colonies were established from polyps provided by Evelyn Houliston (Villefranche-sur-mer). Animals were cultured in 5 glass beakers as described in Chevalier et al (2006), except that artificial seawater was used (36 g/l Reef Crystals®, Aquarium systems).

Scanning electron microscopy

Adult medusae were fixed 1 h at room temperature in 4% paraformaldehyde, washed three times 5 min in PBT and gradually dehydrated in ethanol (20 min washes in 20%, 40%, 60% and 80% EtOH and two final 20 min 100% EtOH washes), then transferred into amyl acetate before critical-point drying. Specimens were mounted on copper stubs with double-sided adhesive tape, coated with 300 A of gold in a Polaron sputtering apparatus and examined on a JEOL JSM 6100 scanning electron microscope at 15 kV. For examination of dissected samples, critical-point dried animals were dissected directly after mounting on double-sided adhesive coating, either by cutting with a microscalpel or by rolling them, tearing and spreading out the external structures and revealing the internal structures.

Transmission electron microscopy and semi-thin histological sections

Clytia tentacle bulbs were isolated with a scalpel blade and forceps, fixed 2 h at room temperature in 6% glutaraldehyde in cacodylate buffer (CB) (0.1 M cacodylate and 1.75% NaCl to correct the osmolarity) and washed three times in CB. Samples were then post-fixed for 45 min in 1% OsO_4 in CB and washed three times in CB. They were progressively dehydrated (EtOH 50%, EtOH 70%, EtOH 95% and twice EtOH 100%, 20 min bathes) and transferred to propylene oxide (20 min in 50% EtOH and 50% propylene oxide, 20 min in 100% propylene oxide). Prior to inclusion in Agar 100 epoxy resin mix (Agar 100 resin kit, Agar scientific: 6 g Agar 100 resin, 4 g DDSA, 2.5 g MNA, 0.38 g BDMA), several incubations were performed in mixtures of Epon resin medium and propylene oxide with increasing resin proportion (2 h 15 in 25% resin, 3 h 45 in 50% resin, one night in 75% resin, 1 h in 75% resin) until incubation in pure resin (1 h in 100% resin, 1 h under vacuum at 50 °C in a small glass cupule to eliminate gas traces). Samples were included and orientated in polyethylene BEEM® moulds previously filled with a thin resin layer and left 48 h at 60 °C for polymerization. Semi-thin and ultra-thin sections were performed with a Diatome diamond histo knife. Ultrathin sections were stained with uranyl acetate and lead citrate before mounting and observation. Semi-thin sections were stained with toluidine blue and mounted in Eukitt medium (Kindler GmbH and Cie, Freiburg, Germany).

TRITC pulse nematocyst staining

The protocol was adapted from Weber (1995). Animals were cultured for 30 min in the dark in 1 μM TRITC (tetramethylrhodamine isothiocyanate, Invitrogen Molecular Probes) in filtered artificial sea water (FASW) under agitation, washed several times in FASW, quickly rinsed in PBT (PBS 1×+0.1% Tween 20) to eliminate as much salt as possible but avoiding an osmotic shock and fixed 10 min in EtOH100. Samples were rehydrated (10 min in EtOH60, 10 min in 30% EtOH, 10 min in PBT), nuclei were stained by a 10-min incubation in 1 μg/ml DAPI (4′,6-diamidino-2-phenylindole) in PBT, rinsed quickly in PBT and medusae were mounted in VectaShield medium. For pulse-chase experiments, TRITC was chased by several washes in FASW, and animals were cultured in FASW in the dark under agitation for 24 h, rinsed in PBT and fixed, rehydrated and mounted as described above.

DAPI poly-γ-glutamate staining

The protocol was adapted from Szczepanek et al. (2002). Samples were fixed for 45 min in 4% PFA in PBS and washed several times in PBS. To stain poly-γ-glutamate (PGA), we incubated samples for 30 min in 140 μM DAPI in PBS. Samples were rinsed several times and mounted in VectaShield. Nuclei blue staining and PGA yellow-orange staining were observed by epifluorescence under DAPI excitation conditions (360 nm).

BrdU pulse labelling assays

The protocol was adapted from Lindgens et al. (2004). Medusae were incubated for 30 min in 5 mM BrdU in FASW, quickly rinsed twice and extensively washed twice for 10 min in FASW. Animals were fixed overnight at 4 °C in 4% paraformaldehyde in FASW and rinsed four times in PBT. DNA was denatured for 30 min in 2N HCl, and samples were rinsed four times for 10 min in PBT. Incorporated BrdU was revealed by immunohistochemistry after an overnight incubation at 4 °C with a 1°/100° diluted mouse anti-BrdU primary antibody (Roche) in PBT+1% BSA, followed by a short rinse and three 10 min PBT washes. The samples were then incubated for 3 h at room temperature in a 1/1000° diluted Alexa 568 anti-mouse antibody (Invitrogen Molecular Probes) in PBT+1% BSA, followed by a short rinse and three 10 min PBT washes. The last wash contained DAPI at 1 μg/ml. Samples were mounted in VectaShield medium. For pulse-chase experiments, animals were cultured 30 min in 5 mM BrdU in FASW, then chased by two rinses and three 5 min washes in FASW, cultured under agitation in FASW containing 100 U/ml penicillin and 0.1 mg/ml streptomycin for 2 to 80 h) and then fixed and treated as described above.

Anti-phospho-histone H3 immunostaining

An anti-phospho-histone H3 (Ser10) antibody (rabbit polyclonal, Upstate (Millipore) 06-570) was used to detect mitotic cells. The corresponding secondary antibody was anti-rabbit Alexa 568 (goat monoclonal, Invitrogen molecular probes A11011). Four percent of paraformaldehyde fixed samples was permeabilized during 10 min in PBS 1% BSA and washed several times for 10 min in PBS 0.1% Triton X-100, and twice for 10 min in PBS 0.01% Triton X-100. Samples were incubated in the primary antibody at a 1/200° dilution in PBS 0.01% Triton X-100 overnight at 4 °C or 2 h at room temperature. Excess antibody was removed by four 15 min washes in PBS 0.01% Triton X-100. Animals were incubated in the corresponding secondary antibody at a 1/1000° dilution in PBS 0.01% Triton X-100, overnight at 4 °C at room temperature in the dark and washed four times in PBS 0.01% Triton X-100. The third wash contained DAPI at 1 μg/ml. Mounting was performed using VectaShield medium and preparations were observed under epifluorescence using a DAPI filter and a Cy3.5 filter (for Alexa 568 detection) on an Olympus BX61 microscope with a Q-imaging Camera.

Gene identification in EST collection

The *Clytia minicollagen 1* and *3-4a*, *NOWA*, *Dkk3* and *Piwi* genes (see Supplementary data) were retrieved by BLAST searches on an EST collection sequenced by the Genoscope (Evry, France) from a *C. hemisphaerica* normalized cDNA library (Chevalier et al., 2006). The library was constructed by Express Genomics (Frederick, Maryland, USA) in pExpress1 plasmids from total mRNA extracted from a mixture of medusa, embryonic and larval stages.

Sequences of the 5 *Clytia* genes were deposited in GenBank under the accession numbers EU195079 (*Chemcol1*), EU024529 (*Chemcol3-4a*), EU195078 (*CheNowa*), EU195080 (*CheDkk-3*) and EU199802 (*ChePiwi*).

Sequence alignment and phylogenetic analyses

For all genes identified by BLAST on *Clytia* ESTs, the orthology group assignation was established by phylogenetic analyses. Other cnidarian and bilaterian sequences were found in GenBank or on www.compagen.org (Hemmrich and Bosch, 2007). Sequences were automatically aligned using CLUSTALW in BioEdit (Tom Hall, Ibis Therapeutics, Carlsbad, CA), and the alignment was corrected manually. Conserved blocks were extracted to perform phylogenetic analyses.

Phylogenetic analyses were carried out by the Maximum-Likelihood (ML) method using the PhyML program (Guindon and Gascuel, 2003), with the JTT model of amino acid substitutions (Whelan and Goldman, 2001). A BioNJ tree was used as the input tree to generate the ML tree. Among site variation was estimated using a discrete approximation of the gamma distribution with 4 rate categories. The gamma shape parameter and the proportion of invariant sites were optimized during the ML search. Branch support was tested with bootstrapping (100 replicates).

Single whole-mount in situ hybridization (ISH)

Protocol was adapted from Chevalier et al. (2006). Digoxigenin antisense probes were synthesized from linearized plasmids using the T7 polymerase as follows: 2 μl Dig labelling mix, 2 μl 10X Reaction buffer, 1 μl Rnasin 40 U and 2 μl T7 polymerase (60–80 U) were added to 13 μl purified linearized DNA template. The RNA probe was precipitated by adding 1/10° volume 3 M sodium acetate and 2.5 volumes ethanol one night at −80 °C, then washed with 70% ethanol and resuspended in 30 μl DEPC water.

Clytia adult and juvenile medusae were let unfed during one night and fixed 1 h in ice cold 3.7% formaldehyde/0.2% glutaraldehyde/PBS at 4 °C. After five 10 min PBT washes, samples were progressively dehydrated and stored at −20 °C in absolute methanol. After several rehydration steps, medusae were incubated in 0.01 mg/ml proteinase K in PBT for 15 min at 37 °C. Digestion was stopped with two washes in PBS containing 2 mg/ml glycine. Samples were gradually transferred to hybridization buffer (HB=5×SSC, 50% formamide, 0.1% Tween) and pre-hybridized for 1 h 30 at 60 °C in HB+0.1% DMSO, 50 μg/ml heparin and 50 μg/ml tRNA. The probe (100 ng/ml) was then added

and hybridization was carried out one night at 60 °C. Excess probe was removed by extensive washes in HB at 60 °C, in 50% HB in PBT at room temperature and finally in PBT. Samples were saturated using blocking buffer in 1X maleic acid (Roche) and incubated in 1/2000° anti-DIG Alkaline phosphatase-coupled antibody (Roche) and washed thoroughly in PBT. Animals were twice incubated 10 min in TMN (100 mM Tris–Hcl pH 8+50 mM $MgCl_2$+100 mM NaCl+10 mM levamisole and 0.1% Tween 20), and alkaline phosphatase activity was revealed by using BM purple reagent (Roche) or Fast Red TR-naphthol reagent (Sigma). Nuclei were counterstained with 1 µg/ml DAPI. Samples were post-fixed (1 h in 4% PFA) and mounted in VectaShield (Vector laboratories). They were observed using a microscope (Olympus BX61) with a Q-imaging Camera using Image Pro plus software ® (Mediacybernetics). Fast Red-revealed samples were observed under epifluorescence (Cy 3.5 filter) and with OptiGrid® Structured-Light System (Qioptiq imaging).

Double whole-mount in situ hybridization

We adapted our simple ISH protocol to double ISH according to Hansen et al. (2000). The protocol was as described above, except that we hybridized samples simultaneously with two different probes: one labelled with digoxigenin, the other with fluorescein. We also performed two rounds of immunostaining and substrate revelation steps: one for each labelling detection. After hybridization and washes, we saturated the samples using Blocking reagent, and we first detected the fluorescein-labelled probe by incubating 2 h in 1/2000 anti-fluorescein Alkaline phosphatase-coupled antibody (Roche) at room temperature. Samples were washed, incubated in TMN and submitted to Fast Red detection. When the signal was sufficiently intense, the reaction was stopped by several PBT washes and by a 100 mM glycine–HCl pH 2.2 10 min incubation at room temperature. Samples were then washes several times in PBT and a new Blocking reagent saturation step was undertaken. We then detected the digoxigenin-labelled probe by incubating 2 h in 1/2000 anti-digoxigenin alkaline phosphatase-coupled antibody (Roche) at room temperature. Medusae were washed, incubated in TMN and submitted to BM purple revelation. The reaction was stopped by several PBT washes, and nuclei were stained with DAPI. Samples were mounted in VectaShield and analyzed by transmission and epifluorescence as described above.

Results

Minicollagen gene expression identifies tentacle bulbs as the major nematogenesis sites in Clytia *medusae*

To determine the sites of nematogenesis in *Clytia* medusae, we examined the expression of minicollagens, small collagen-like proteins identified in *Hydra* as the major component of the nematocyst wall (Kurz et al., 1991). We performed whole-mount *in situ* hybridization to detect mRNAs from two of three minicollagens genes identified in *Clytia*, *mcol1* and *mcol3-4a*. Both revealed the same two sites of nematogenesis: the very proximal part of the manubrium (the structure bearing the mouth) and the tentacle bulbs (Fig. 1A). The most intense

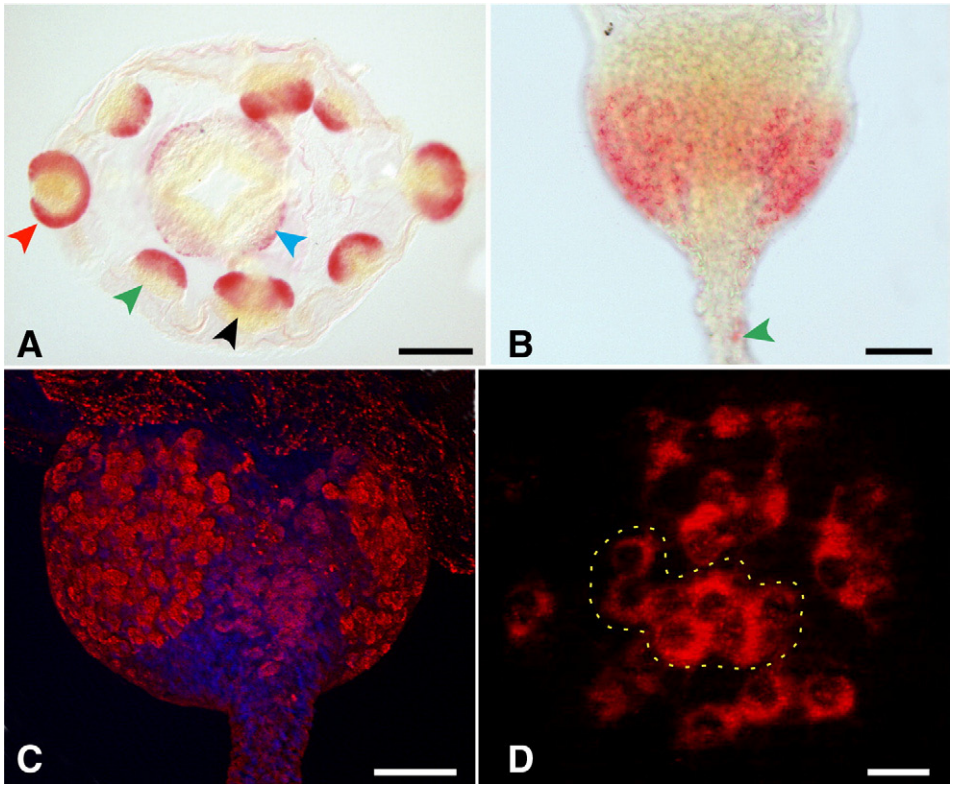

Fig. 1. *Minicollagen* transcript localization identifies the tentacle bulbs as major nematogenesis sites of *Clytia* medusa. (A–D) Whole-mount *in situ* hybridizations (FastRed development). (A) *minicollagen 1* mRNA localization on adult medusa, subumbrella side. Staining on mature tentacle bulbs (black arrowhead for side view and red arrowhead for apical view), developing bulb buds (green arrowhead) and manubrium basis (blue arrowhead). (B) Close-up of *minicollagen 3-4a* RNA localization on the tentacle bulb (external side). Green arrowhead: isolated cells in the tentacle. (C–D) Close-up of *minicollagen 3-4a*-expressing-cells in the tentacle bulb (external side), Z projection of OptiGrid optical sections (Cy 3.5 filter). (C) The staining shape corresponds to an externally interrupted crescent, composed of round to ovoid cells. Nuclei are stained with DAPI (in blue). (D) Nematoblasts are associated in clusters. A cluster is encircled in yellow. Scale bars: A, B: 250 µm; C: 25 µm; D: 2,5 µm.

staining was found on the latter (Fig. 1B), indicating that the tentacle bulbs are the major sites of nematogenesis in *Clytia*. *Minicollagen* expression was also detected in isolated cells in the tentacle (Fig. 1B), but not in mature nematocytes, either in the tentacles or the manubrium lips.

A crescent-shaped nematogenesis zone in the Clytia *tentacle bulb ectoderm*

Close analysis of the tentacle bulb revealed the cells expressing *mcol3-4a* as numerous round cells in the ectodermal layer of the bulb (Fig. 1C) and a few isolated cells in the tentacle (Fig. 1B). The tentacle bulb cells were grouped in clusters of up to around 8 cells (Fig. 1D). The *minicollagen* expressing zone formed a crescent around the bulb rather than a complete ring, the *in situ* staining being interrupted on the external side of the bulb (visible on the apical view of a stained bulb on Fig. 1A, red arrow).

Scanning electron microscopy (SEM), phalloidin staining and toluidine blue staining of semi-thin sections were performed to clarify the localization of the nematogenic area (Fig. 2). The bulbs exhibited clear bilateral symmetry associated with a contrasted external morphology of the inner (adaxial) and outer (abaxial) faces of the bulb with respect to the symmetry axis of the animal (Figs. 2A and B). The outer side of the bulb is flattened whereas the internal side has a thickened morphology. Moreover, the tentacle insertion site is slightly off center towards the external side. A group of naturally fluorescent cells was detected in a triangular area on external side of the bulb, providing a convenient landmark (Fig. 2B). Optical sections of phalloidin-stained bulbs demonstrated the marked thickening of the ectoderm of the tentacle bulb (TBE) compared to that of the umbrella and tentacle regions (Fig. 2C). DAPI staining of nuclei revealed that this thickening reflected an increased number of cells rather than larger cell size (Fig. 2C). In the distal-most part of the bulb and in the most proximal part of the tentacle, the ectodermal phalloidin staining was more intense, suggesting that cell in these regions have thickened actin cortices (Figs. 2C and D). On transverse semi-thin toluidine blue sections of the bulb, nematoblasts are easily distinguishable from the other cell

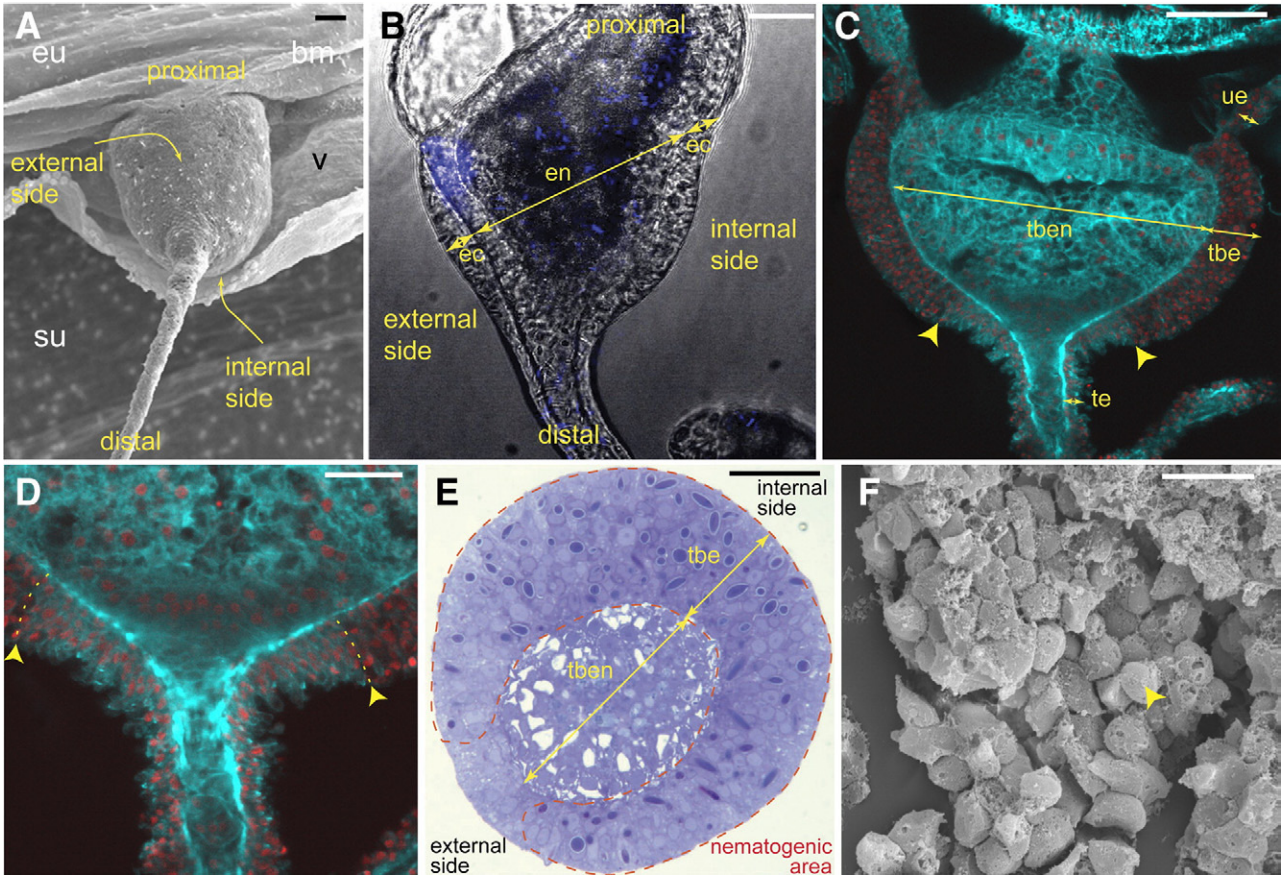

Fig. 2. Morpho-anatomy of the tentacle bulb. (A) Scanning electron microscopy (SEM) pictures of a tentacle bulb (frontal view, external side) showing its insertion on exumbrellar tissues (eu) on the bell margin (bm), and the relative positions of the velum (v) and the subumbrella (su). This insertion surface defines the most proximal part of the bulb, the most distal point being the tentacle tip. (B) Side confocal view of a live isolated tentacle bulb, superposition of a DIC transmission picture and of the natural fluorescence (in blue). en: endoderm, ec: ectoderm. (C–D) Confocal optical section of phalloidin stained (cyan) bulb with DAPI stained nuclei (red), false colors. Frontal view. (C) The tentacle bulb ectoderm (tbe) appears very thick compared to the umbrella ectoderm (ue) and the tentacle ectoderm (te). tben: tentacle bulb endoderm. The arrowheads highlight the frontier of the more intensely stained area. (D) The ectoderm of the distal area of the bulb and the proximal area of the tentacle presents a more intense phalloidin staining (close up). (E) Toluidine blue-stained transverse semi-thin section of a bulb (at the median level). tbe: tentacle bulb ectoderm, tben: tentacle bulb endoderm (revealing the tentacle axis). (F) Dissected tentacle bulb ectoderm on SEM (internal view) revealing almost only nematoblasts (one of them is marked by the arrowhead). Scale bars: A, B, C, F: 25 μm; D: 10 μm; F: 5 μm.

types present (notably myoepithelial cells), from the early nematoblast stage, by the distinct coloration of the cytoplasm. Nematocysts at various stages of differentiation appeared as prominent blue spots (Fig. 2E). From examining transverse sections, it was clear that although most of the TBE is nematogenic, there is a narrow, thinner segment at the center of the external side that contains almost no nematoblast (Fig. 2E), corresponding to the interruption of *mcol3-4a* expression (Fig. 1C and red arrow on Fig. 1A). SEM observations of dissected bulbs showed nematoblasts as spherical cells concentrated in the ectoderm (Fig. 2F), whereas the later stages appeared more ovoid or spindle shaped. Taken together, these observations characterize the tentacle bulb ectoderm as a region specialized for tentacular nematogenesis.

Proximo-distal regionalization of the nematogenic TBE

TEM and histological sections were used to examine the distribution of nematogenesis stages within the nematogenic TBE. The following stages were identified by TEM, according to previous descriptions (Holstein, 1981) (Figs. 3A–F): (i) undifferentiated, interstitial cells (either stem cells or early committed nematoblasts) characterized by a high nucleocytoplasmic ratio and a large nucleus with a developed nucleolus (Chapman, 1974) (Fig. 3A); (ii) Early differentiating nematoblasts, with the nascent capsule detectable as a highly electron lucent cytoplasmic spherical element and cytoplasm filled with rough endoplasmic reticulum (Fig. 3B); (iii) later differentiation stages containing a larger developing capsule and a thread forming in the cytoplasm visible as cytoplasmic dense elements (Fig. 3C); and (iv) nematoblasts with a full-sized capsule containing an internal coiled thread differentiated into a large shaft area and a thinner tubule (Figs. 3D–F). Within this category, we could distinguish capsules with a more electron-lucent matrix (Fig. 3F compared to 3E), corresponding to mature nematocytes as found in the tentacles (data not shown).

The distribution of nematogenesis stages was determined on serial toluidine blue stained semi-thin transverse sections (Fig. 3G, see also Supplementary data). We considered only those stages that could be unambiguously recognized on the basis of the TEM analysis: early forming capsules (corresponding to the stage on Fig. 3B), differentiating capsules (corresponding to the stages on Figs. 3C–E) and mature nematocytes (corresponding to the stage on Fig. 3F). Early nematogenesis stages were mainly found in the proximal-most part of the TBE, progressively disappearing from medial and distal sections. Very few late stages were found in proximal regions, but they were found in majority in the distal part of the TBE. Differentiating nematoblasts were thus mostly found in the median zone of the TBE. There is thus a clear regionalized organization of nematoblast stages along the proximo-distal axis of the bulb. There is not a strict segregation of stages but rather a graded distribution of each stage. For example, mature nematocytes are not exclusively located at the distal extremity of the bulb and in the tentacle, a few mature nematocytes being detected even in the proximal half of the bulb (Fig. 3G). On distal transverse sections, a differential distribution of nematoblast stages between the center and the periphery of TBE was also observed, the more mature stages being closer to the mesoglea (Fig. 3H). Undifferentiated cells were localized on the most proximal transverse sections. Here, we did not find nematoblasts with a developing capsule, but we found a majority of undifferentiated cells with a dark blue cytoplasm (Fig. 3I) (as well as a large nucleus and a large nucleoli, data not shown). Moreover, on both sides of the bulb basis, we observed two symmetric groups of undifferentiated cells with lighter cytoplasm (Fig. 3I) (and a large nucleus, data not shown).

Fluorescent labelling techniques were used to determine the distribution of particular stages of late nematogenesis: TRITC that selectively labels nematoblasts during a short time frame at the end of nematoblast differentiation (later than *minicollagen* expression; Weber, 1995), and DAPI staining to detect poly-γ-glutamate, present in late stages of differentiation and fully mature nematocysts (Fig. 3K). TRITC labelling localized late differentiating nematoblasts to a restricted area of the most distal part of the bulb and the most proximal part of the tentacle (Fig. 3J). Orange DAPI staining overlapped with the area of TRITC staining and also decorated the mature tentacular nematocytes.

Taken together, these various observations allow us to define four areas in the TBE with distinct proportions of nematoblast stages (Fig. 3L). The very thin (about 10 μm) proximal-most region of the TBE ("α" region) contains only undifferentiated cells and almost no maturing or mature nematocytes, with lighter-staining cells being grouped on each side. The "β" region comprises most of the TBE (excluding the basal-most and distal-most areas) and contains cells at various stages of differentiation. The "γ" region, highlighted by TRITC staining all around the distal bulb and the proximal tentacle, contains mainly the latest stages of capsule maturation. Finally, the "δ" region is rest of the tentacle (except its proximal-most area), and contains only mature nematocytes (stained with DAPI but not with TRITC).

Active cell proliferation in the Clytia TBE

Cell proliferation in the TBE was examined by BrdU incorporation (to detect DNA synthesis) and immunochemistry with an anti-phospho-H3 antibody (to detect mitotic chromatin). The tentacle bulbs were found to be the major areas of mitosis and BrdU incorporation within the medusa (not shown). A high density of mitotic cells was found in a crescent-shaped region of the TBE, corresponding to the nematogenesis area, indicating intense division activity among nematoblasts (Fig. 4A). Within this area, anti-phospho-H3 staining intensity was uniform suggesting homogeneous cell division between the various zones. After a 30-min pulse incubation, BrdU incorporation was also detected in the nematogenesis area (Fig. 4B). DNA replication appears very active in this region since a 5-min incubation in BrdU was sufficient to give strongly detectable incorporation (data not shown). A closer analysis showed that incorporation was slightly greater in the α and the proximal β regions of the bulb (Fig. 4B). Altogether, these results suggest

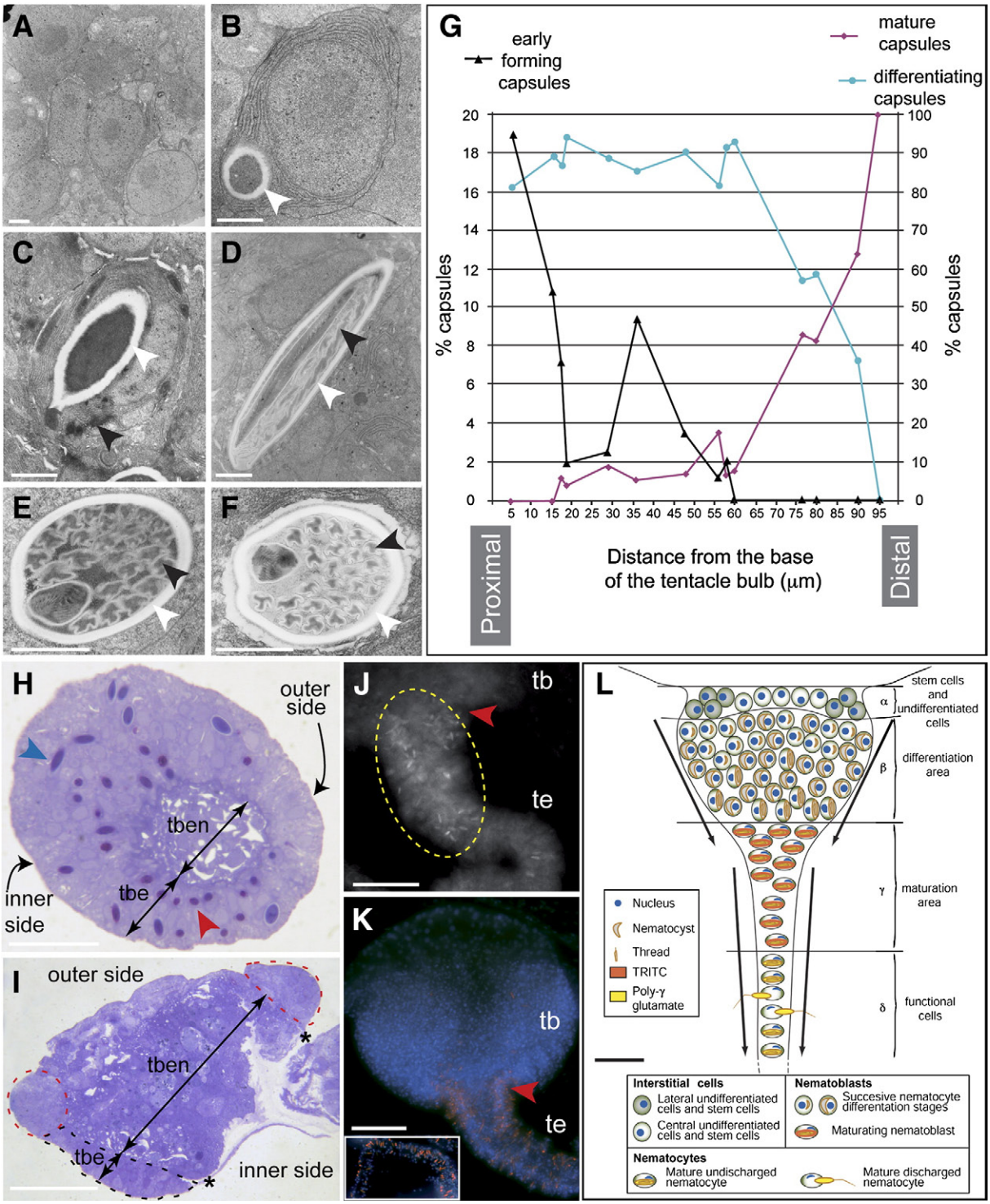

Fig. 3. The nematogenesis stages are proximo-distally distributed in the tentacle bulb ectoderm. (A–F) Transmission electron microscopy pictures of nematoblast stages in the TBE. White arrowheads: capsules; black arrowheads: thread. (A) Interstitial cells. (B) Early nematoblast with a small developing capsule. (C) Nematoblast with a developing capsule and an external thread differentiating in the cytoplasm. (D) Nematocyte with a mature capsule. (E–F) Transition from a nearly mature capsule with an electron dense matrix (E) to a mature capsule with an electron lucent matrix (F). (G) Graph showing the percentages of three stages of capsule maturation along the proximo-distal axis. Two different ordinates for the percentage of early forming nematoblasts on the left and for the percentage of differentiating and late maturating nematoblasts on the right. (H–I) Toluidine blue-stained transverse semi-thin sections of a bulb. tbe: tentacle bulb ectoderm; tben: tentacle bulb endoderm. (H) Section in the intermediate region between the bulb and the tentacle showing mature capsules (in purple, red arrow) and immature capsules (in blue, blue arrow). (I) Most proximal section with undifferentiated cells, showing two lateral areas with cells displaying an interstitial cell phenotype with a light cytoplasm (red dotted lines) and an inner area with cells with the same phenotype but with a blue cytoplasm (black dotted lines). Asterisks delimit an area where a part of the section is not present (the most proximal end of the isolated bulb was reached). (J) TRITC staining revealing nearly matures capsules after 30 min of incubation. (K) DAPI staining (nuclei stained in blue and poly-γ-glutamate containing capsules in orange). Small box: view of the tentacle. On J and K, arrowhead: tentacle insertion site on the bulb. tb: tentacle bulb; te: tentacle. (L) Synthetic diagram illustrating the proximo-distal distribution of nematogenesis stages in the tentacle bulb ectoderm. Scale bars: A–F: 1 μm; H–L: 25 μm.

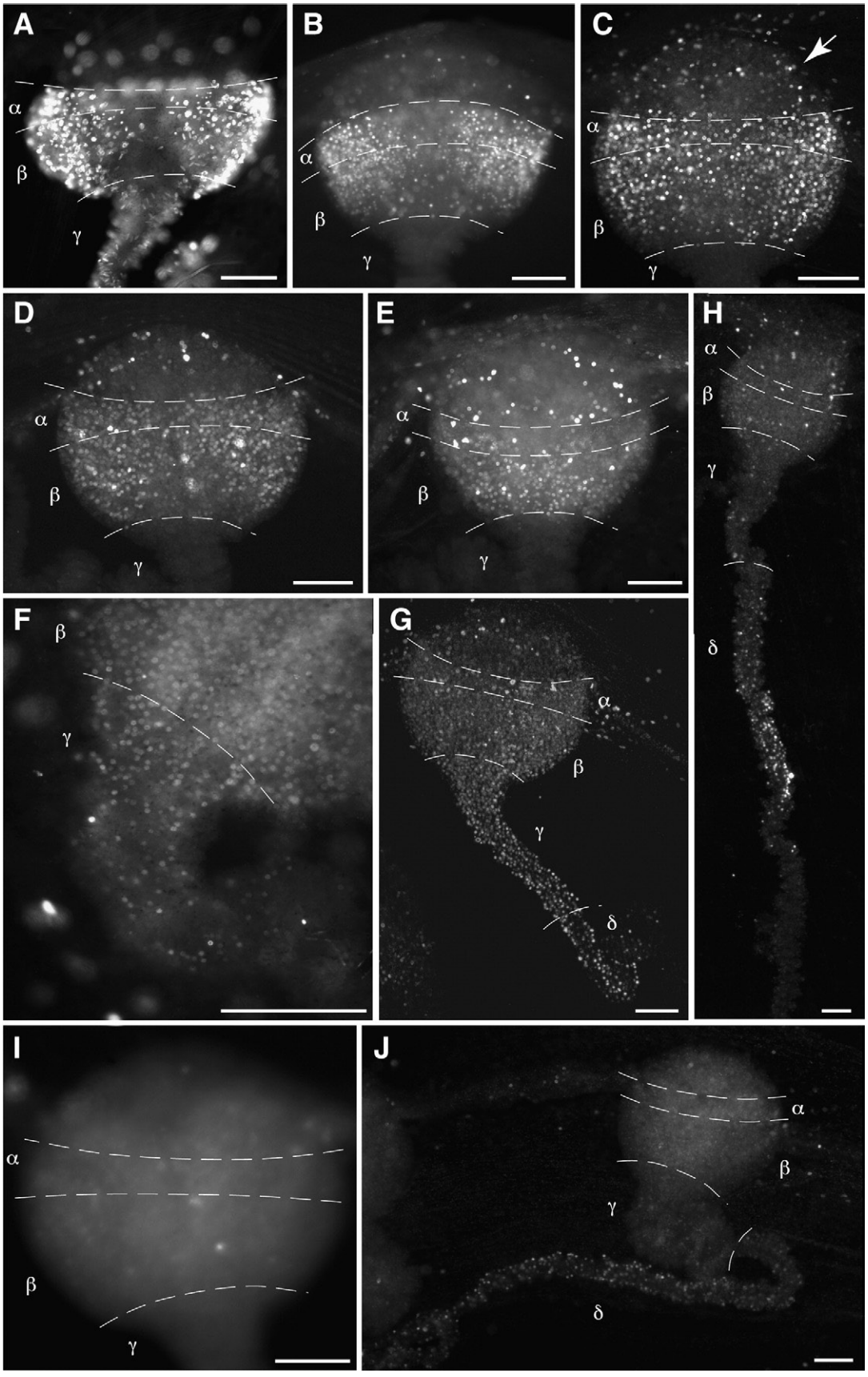
A
α
β
γ
B
α
β
γ
C
α
β
γ
D
α
β
γ
E
α
β
γ
H
α
β
γ
δ
F
β
γ
G
α
β
γ
δ
I
α
β
γ
J
α
β
γ
δ

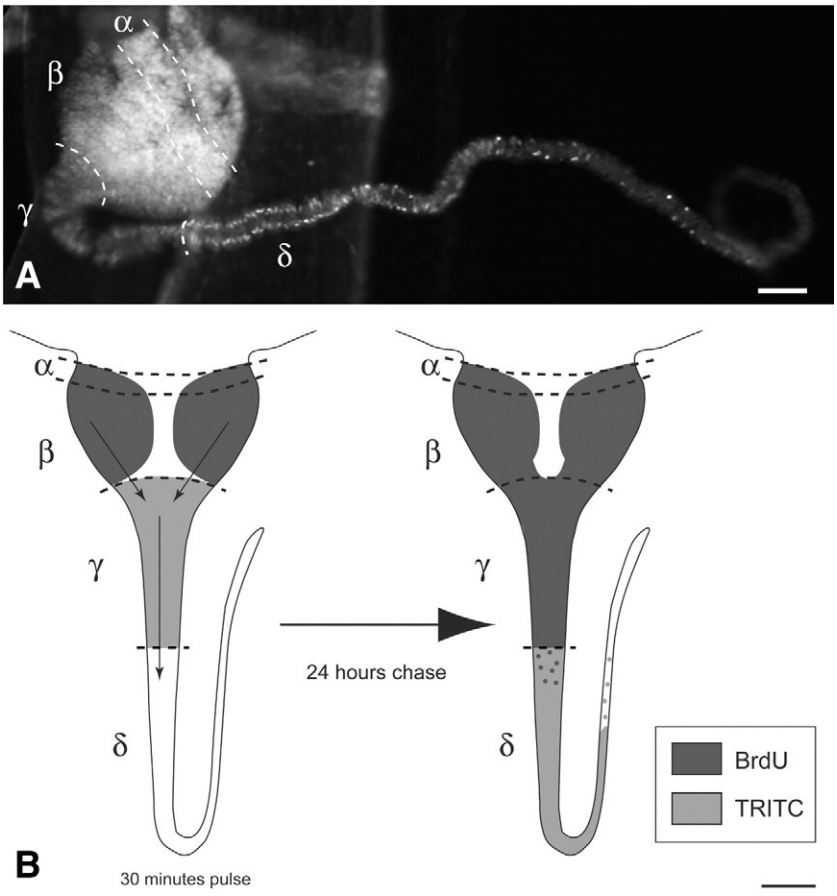

Fig. 5. Capsule movements in the TBE. (A) TRITC staining after 30 min incubation and 24 h chase. The background staining is due to the weak staining of all membranes by TRITC. (B) Scheme comparing TRITC and BrdU pulse/chase results. Scale bar: 25 μm.

that mitotic division occurs at many of the nematogenesis stages previously identified in the TBE crescent-shaped area.

Rapid displacement of TBE cells into the tentacle

To determine the fate of cells dividing in the TBE, we performed BrdU pulse/chase experiments. After 30 min incubation in BrdU, medusae were cultured 1 to 72 h in BrdU-free seawater, fixed, and the BrdU was detected by immunohistochemistry (Figs. 4C–J). BrdU-labelled nuclei were still located in the TBE nematogenic area after 2 or 8 h of chase (Figs. 4C, D). However, after 2 h, some cells had become displaced from the bulb to the bell margin (Fig. 4C, arrow). After 10 h, a slight shift of the bulk of the labelled nuclei towards the distal part of the β region could be detected (Fig. 4E); and after 16 h, labelled nuclei were also detectable in the γ region (Fig. 4F). Thereafter, they were found in progressively more distal positions in the tentacle (Figs. 4G–I). After 24 h of chase, labelled nuclei extensively covered the γ region and the proximal δ region of the tentacle (Fig. 4G); after 48 h, they had totally evacuated the bulb and began to populate the δ region (Figs. 4H, I); and after 72 h labelled nuclei had reached the tentacle tip (Figs. 4J). Scattered stained nuclei were often found more distally than the main group of stained nuclei. After around 8 h, the TBE cells progressively leave the bulb and massively populate the tentacle. To show directly the presence of nematocytes among the cells moving from the TBE into the tentacle, we used the live TRITC staining technique to label the wall of late, maturing nematoblasts. Animals were incubated in TRITC for 30 min, then washed and cultured for 24 h in TRITC-free seawater. During this period, labelled nematocysts moved towards the δ region, populating almost the entire length of it, except the γ area that was initially stained after 30 min TRITC incubation (Fig. 5A). Late differentiating, post-mitotic, nematoblasts are thus included in a massive cellular flow from the tentacle bulb to the tentacle.

Fig. 4. Cell division and nuclei movements in the TBE. (A) Anti-phosphoH3 immunolocalization in the TBE. (B) Thirty-minute pulse staining with BrdU revealing nuclei undergoing DNA replication in the TBE. (C–J) Pulse/chase experiments after 30 min incubation in BrdU. (C) Two-hour chase. Arrow: isolated nuclei near the bell margin. (D) Eight-hour chase. (E) Ten-hour chase. Stained nuclei are now concentrated in the distal β zone. (F) Sixteen-hour chase. Stained nuclei have reached the γ zone. (G) Twenty-four-hour chase. Stained nuclei cover one third of the tentacle. (H) Forty-eight-hour chase. Stained nuclei populate the middle region of the tentacle. (I) Forty-eight-hour chase. High magnification of the bulb showing the absence of stained nuclei. (J) Seventy-two-hour chase. Stained nuclei cover the most distal part of the tentacle. On all pictures, the junctions between the four areas of the bulb are marked with a dotted line. Scale bars: 25 μm.

Overlapping expression domains of nematogenesis genes in the TBE

Studies in *Hydra* and other cnidarians have characterized a number of genes whose expression is associated with different steps of nematogenesis. In addition to *minicollagens*, we identified three of these genes from a *Clytia* EST collection and analyzed their expression: the stem cell marker gene *Piwi* (previously studied in *Podocoryne*, Seipel et al., 2004), the late regulator gene *Dkk3* (Fedders et al., 2004) and the structural

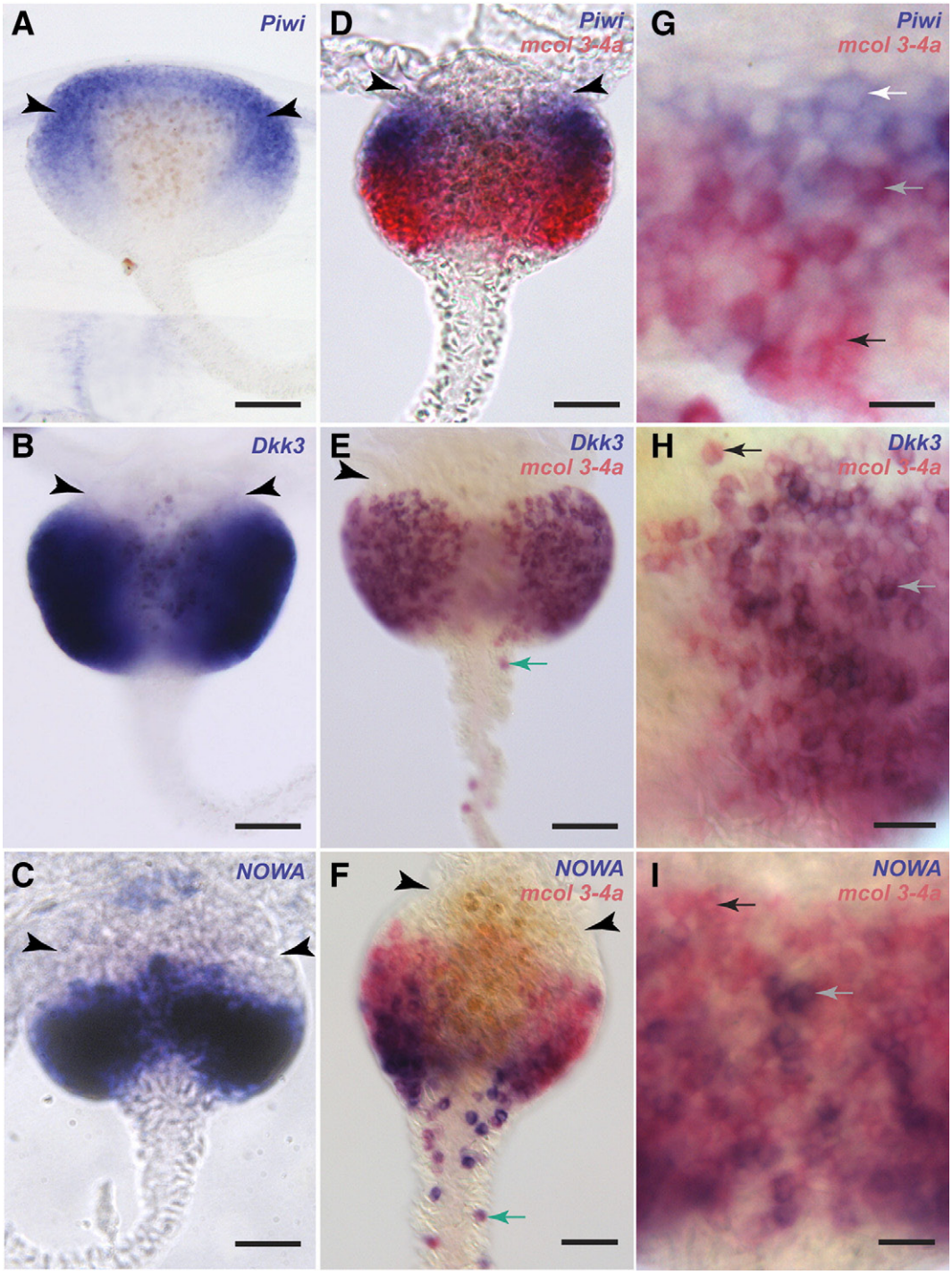

Fig. 6. Sequential gene expression territories in the TBE. Bulbs are viewed from the outer side. (A–C) Single *in situ* hybridizations (BM purple development). (A) *Piwi*. The bulb is slightly turned towards the proximal end, so that the continuity of the staining on the inner face is visible. (B) *Dkk3*. (C) *NOWA*. (D–F) Double *in situ* hybridizations, *minicollagen 3-4a* developed with Fast Red in each case and the second probe with BM purple. (G–I) Details of double *in situ* hybridizations. (D, G) *Piwi*. (E, H) *Dkk3*. (F, I) *NOWA*. Scale bars: A–F: 25 μm; G: 5 μm; H, I: 10 μm. Arrowheads: tentacle bulb insertion site on the umbrella. Green arrows: isolated cells in the tentacle. White arrows: cells expressing only the probe developed with BMpurple. Black arrows: cells expressing only *minicollagen 3-4a* (Fast red). Grey arrows: cells expressing both markers.

gene *NOWA* (Engel et al., 2002) (see Materials and methods and Supplementary data for gene identification procedure and phylogenetic analyses). All three genes were expressed in the TBE crescent-shaped nematogenic area, but in a sequential manner along the proximo-distal axis, in accordance with the cellular characterization of nematogenesis described above. *Piwi* was strongly expressed in the proximal TBE, in the α region and in two lateral areas in the proximal part of the β region. This gene was also expressed in a more diffuse manner in the center of the proximal part of the β area (Fig. 6A). *Dkk3* was expressed through the entire β region (Fig. 6B). Finally, *NOWA* was expressed weakly in the proximal β region and strongly in the distal part of the β as well as in some isolated cells in the tentacle (Fig. 6C). NOWA expressing cells were distributed in clusters and sometimes aligned along the proximo-distal axis (data not shown).

Double *in situ* hybridizations positioned the expression domains with respect to *mcol3-4a* expression. We found that *Piwi* coexpressed with *mcol3-4a* in two symmetric lateral patches of cells in the proximal part of the β region, as well as a narrow stripe of cells in the central area (Figs. 6D and G). However, in the α region, there were a majority of cells expressing *Piwi* alone with few cells coexpressing the two genes. *Dkk3* coexpressed with *mcol3-4a* in all cells except for a few isolated *mcol3-4a*-positive cells in the tentacle and some cells near the lateral extremities of the crescent (Figs. 6E, H). The *Dkk3/mcol3-4a* domain corresponds to the β region. *NOWA* also coexpressed with *mcol3-4a* in part of the β region, the majority of *NOWA*-expressing cells occupying the distal part of the β area, and a small proportion of *NOWA*-expressing cells also occurring more proximally and in the tentacle (Figs. 6F, I). *NOWA*-positive cells were found to contain a more developed capsule than cells expressing only *mcol3-4a*, but the capsules were probably immature in these cells as they deformed upon fixation (not shown).

Discussion

The Clytia tentacle bulb is a specialized structure dedicated to the production of tentacle nematocytes

The ectoderm of the tentacle bulb is a specialized territory of the medusa that functions as a nematocyte production center, in contrast with diffuse nematogenesis in cnidarian polyps. In *Hydra*, interstitial stem cells are distributed throughout the ectoderm and endoderm, and clusters of nematoblasts at all stages of differentiation are scattered along the length of the body column ectoderm, except its basal-most and apical-most extremities (David and Challoner, 1974; David and Gierer, 1974; Fujisawa et al., 1986; Bode, 1996). Given that the tentacle ectoderm is the final destination of most mature nematocytes, differentiated cells must undergo migration along the column from their differentiation sites to the tentacles (Bouillon, 1994). In colonial hydrozoans like *Hydractinia*, nematogenesis is thought to occur in the basal stolons before nematocytes migrate towards individual polyps (Teo et al., 2006). Our *in situ* hybridization analyses for molecular markers of nematogenesis demonstrated that in the *C. hemisphaerica* medusa nematogenesis is essentially concentrated into two areas: the inner TBE and a distinct region at the base of the manubrium ectoderm. The latter site produces nematocytes of the mouth and manubrium, whereas the TBE generates tentacle nematocytes. Mature nematocytes are also present in others locations in the medusa, the bell margin and the exumbrella (Östman, 1979); however, the absence of detectable nematogenesis marker expression and TRITC labelling in these area indicates that they are not produced locally. The BdrU pulse-chase analyses show that there are nuclei movements from the tentacle bulb to the bell margin. Nematoblasts or nematocytes could be part of these moving cells, and the bell margin nematocytes could thus possibly be also produced in the TBE. Further experiments will be needed to investigate the origin of exumbrellar nematocytes.

The existence of a graded progression of nematoblast stage populations along the TBE, from the base of the bulb to the site of tentacle insertion, is remarkable. No such spatio-temporal ordering of nematogenesis exists in the previously studied models, particularly *Hydra*. We hypothesize that this ordered progression is a consequence of (i) the spatial restriction of stem cells at the bulb base, as revealed by histological sections (Fig. 3H) and localization of *Piwi*$^{+}$/*mcol3-4a*$^{-}$ transcripts (Figs. 6A, D, G) and (ii) the continuous translocation of differentiated stages towards the tentacle. The degree of spatial restriction of nematogenesis stages along the bulb axis is sufficient for genes involved in distinct steps of the process to be expressed in staggered crescents, located more basally for earlier genes and more distally for later genes (Fig. 6). Stage segregation along the bulb axis was not, however, perfect (Figs. 3G, L). Likely explanations include a certain amount of mixture between cells within the TBE, some degree of heterogeneity between clusters in the timing of commitment and nematogenesis steps, and variability in the rate of cell translocation towards the tentacle. The presence of a few mature nematocytes within the β region could represent a subpopulation dedicated to a defensive role on the TBE surface.

From the evolutionary point of view, tentacle bulbs represent an innovation (synapomorphy) of the Hydroidolina clade (Collins et al., 2006), a large group that comprises the vast majority of hydrozoan species. Similar expression pattern of the *Piwi* homologue *Cniwi* in the tentacle bulb of *Podocoryne* (Seipel et al., 2004) compared to *Clytia* suggests that the basic features of TBE nematogenesis are conserved among Hydroidolina despite evolutionary divergence between these two species. Non-Hydroidolina hydromedusae (Trachylina) are devoid of tentacle bulbs and their nematogenesis area extends around the whole bell margin (in the so-called “Nesselring”) (Bouillon, 1994). Thus, the acquisition of tentacle bulbs in an ancestor of Hydroidolina resulted in a higher spatial restriction of tentacle nematogenesis.

Dynamics of nematogenesis in the TBE

We were able to recognize all nematogenesis stages previously described in *Hydra* and other Cnidaria (Westfall, 1966; Holstein, 1981) in the *Clytia* TBE. As in other

hydrozoans like *Hydra* (Slautterback and Fawcett, 1959), *Obelia* (Westfall, 1966) or *Podocoryne* (Boelsterli, 1977), the nematoblasts were found to be grouped in clusters. In *Hydra*, it has been shown that nematogenesis requires several mitosis steps during early stages and an additional terminal division seems to occur after capsule formation (Campbell and David, 1974; Engel et al., 2002). In *Clytia*, we observed from our anti-H3 and BrdU experiments a broad proliferation zone covering the whole TBE crescent, with slightly more BrdU incorporation detected in the proximal area, suggesting that nematoblasts divide throughout all early stages as in *Hydra*, but possibly also in later stages of differentiation with a developing nematocyst. In *Podocoryne*, tentacle bulbs have also been shown to be intensive proliferation sites, as well as the manubrium and the bell margin (Spring et al., 2000).

The total duration of nematogenesis in *Clytia* is clearly shorter than in *Hydra*. We showed that a dividing cell in the proximal-most area of the bulb, where cells express the stem cell marker *Piwi* will reach the tentacle after 1 to 2 days. In comparison, in *Hydra* it was shown by [3H] incubation that nematoblasts differentiate within 5 to 8 days depending on the nematocyst type (5–7 days for desmonemes and isorhizas; 7–8 days for stenoteles). The timing difference between nematocyte types is thought to be due to a "lag phase" during which stenoteles undergo a special maturation step before migration (Weber, 1995). *Clytia* medusae are known to possess a majority of small oblong nematocytes, known as microbasic-b-mastigophores, in addition to a minority of larger and more spherical nematocytes, termed atrichous isorhiza (Östman, 1979). Within the TBE, we followed the nematogenesis of the first category, which is mostly used for prey capture, as are *Hydra* stenoteles. As for stenoteles in *Hydra*, colonization of the tentacles by nematocytes in *Clytia* following BrdU incorporation involved a latent phase, the cells moving into the tentacle after 8 to 12 h. This phase of latency could involve a tissue reorganization step necessary to elaborate the final tentacle tissue structure. Within the TBE, nematoblasts are numerous in the interstices between adjacent myoepithelial cells, whereas in the tentacle there is only one layer of interstitial nematocytes. The intense phalloidin staining in the γ region (Fig. 2D) could reflect tissue remodelling in the "bottle neck" zone.

Stem cells and Piwi *expression in TBE*

The narrow band, or "α" region, at the base of the TBE, in which a majority of cells express the *Clytia Piwi* homologue but not the differentiation marker *mcol3-4a*, is likely to comprise a population of stem cells. Histologically this region was found to contain undifferentiated cells with a high nucleocytoplasmic ratio. The *Piwi* gene is a widely conserved stem cell marker throughout multicellular eukaryotes, including *Drosophila* (Lin and Spradling,1997; Cox et al., 1998), annelids (Rebscher et al., 2007), platyhelminths (Rossi et al., 2006; Reddien et al., 2005), vertebrates (Cox et al., 1998; Cikaluk et al., 1999; Tan et al. 2002), sea urchins (Qiao et al., 2002) and the cnidarian *Podocoryne* (Seipel et al., 2004). A homologue has even been identified in the ciliates *Tetrahymena* (Mochizuki et al., 2002) and *Stylonychia* (Fetzer, 2002). In all studied Bilateria, the Piwi protein is crucial for germ stem cell maintenance and division as well as somatic stem cell maintenance because it silences gene expression by RNA interference (Lin and Spradling, 1997; Cox et al., 1998; Lingel and Sattler, 2005).

In the *Clytia* TBE*, Piwi* was expressed not only in stem cells but during the first steps of nematogenesis, as show by coexpression with *mcol3-4a* in the β region and in a few isolated cells in the α region. Coexpression of *Piwi* and *mcol3-4a* was extended in two symmetrical patches located laterally in the proximal part of the β region. The *Piwi* staining was more diffuse in the central part of the proximal β area, where it also partly overlapped with *mcol3-4a* pattern. Coexpression of *Piwi* and *mcol3-4a* suggests that after commitment, early nematoblasts initially maintain *Piwi* expression but then progressively lose it. This could reflect a progressive loss of stem cell potential. The wider staining in the lateral areas compared to the centre could be explained by the number of $Piwi^{+}/mcol3\text{-}4a^{-}$ cells that is more important in the lateral areas, consistent with the two patches observed on semi-thin sections (Fig. 3I, see also Supplementary data). In consequence, the number of proliferating and differentiating cells is higher in the lateral areas.

An antagonistic Frizzled family receptor *CheFz3* is also expressed in lateral parts of the tentacle bulb base, while the classical Frizzled *CheFz1* is expressed more widely (Momose and Houliston, 2007). The Wnt pathway may thus be involved in regulating early steps of *Clytia* nematogenesis, for instance the balance between proliferation and commitment of nematoblast precursors, since the Wnt pathway has been implicated in the control of interstitial cell proliferation in *Hydractinia* (Teo et al., 2006)

Nematocyte differentiation markers in the TBE

We showed that the expression of four homologues of *Hydra* nematocyte differentiation markers was conserved in *Clytia* tentacle bulb nematogenesis, and that their relative expression patterns were consistent with our spatio-temporal model. *mcol1 and mcol3-4a* were mostly expressed in the β crescent-shaped differentiation area. *Dkk3* almost totally overlapped with *mcol3-4a*, whereas *NOWA* was expressed in a subset of *mcol3-4a*-positive cells, mainly in the distal part of the β area, comprising a majority of late differentiating nematoblasts with a well-formed but still immature capsule.

This mRNA distribution in differentiating nematoblasts was coherent with published data on *NOWA* and *Dkk3* expression timing and on NOWA function, even if the absence of published double *in situ* hybridizations with *minicollagens* precludes estimation of the exact overlap between the expression of these genes in *Hydra*. In *Hydra*, the NOWA protein was shown to be involved in minicollagen condensation and cross-linking (Engel et al., 2002), leading to capsule wall maturation, at the end of the nematogenic process. Consistently, *NOWA* and *mcol3-4a* mRNAs are mostly coexpressed in the distal differentiation area, and more proximally than the TRITC-stained nematocysts (revealing nematoblasts undergoing the wall maturation step).

The *Dkk3* gene belongs to the *Dkk3 Dickkopf* subfamily. Contrary to *Dkk 1*, *2* and *4*, *Dkk3* genes have not been shown to be implied in the Wnt pathway, and their function remains to be investigated (Fedders et al., 2004). The *Hydra Dkk3* gene is expressed in differentiating nematoblasts in the body column, a pattern that parallels the *Clytia* staining in the β zone, which contains a majority of differentiating stages. In *Hydra*, *Dkk3* is also expressed in isolated, mature migrating nematocytes near the tentacle. In *Clytia*, these cells would be predicted to lie in the γ zone, but no *Dkk3*-positive cells were detected in this region, indicating that *Dkk3* expression in *Clytia* stops earlier than in *Hydra.*

The transcription factor-coding *FoxB* gene, implicated in neurogenesis in vertebrates, has also been reported to be expressed in the proximal β area in a crescent-shaped pattern (Chevalier et al., 2006). As *Zic* or *CnASH*, the expression of *FoxB* in nematoblasts (if it is confirmed) would thus be reminiscent of the expression of *FoxB* during neurogenesis in Bilateria (Odenthal and Nusslein-Volhard, 1998; Gamse and Sive, 2001; Mazet and Shimeld, 2002). Moreover, *FoxB* was also expressed in several *Clytia* medusa sense organs (Chevalier et al., 2006): the statocysts, gravity-sensing organs linked to the neural coordination system of hydromedusae as well as in the larval endoderm, and possibly in the gonad photoreceptors. In addition, it is expressed in the endoderm of the planula, in particular at the posterior pole, where the nematocytes and neurons are committed. Therefore, the expression of *FoxB* in cnidarian neuron-related cells could represent an ancestral legacy; alternatively, the gene could have been secondarily recruited.

No differentiation markers have yet been found to be specifically expressed in the γ region. In contrast the maturation markers TRITC and DAPI were able to stain nematoblasts and nematocytes in this area. Weber (1995) observed that in *Hydra* nematocysts lose their TRITC staining ability precisely when the final osmotic pressure is reached in the matrix, i.e. when PGA accumulation has reached its maximum. Our results are consistent with this observation because we observed (i) an area of late maturating nematoblasts stained with both TRITC and DAPI, and containing a maturating cyst wall and a poly-γ-glutamate-filling matrix (the γ area), and (ii) more distally in the rest of the tentacle (the δ area), only mature nematocytes whose cyst wall had lost the ability to fix TRITC but whose cyst matrix was brightly stained with DAPI.

minicollagen and *NOWA in situ* hybridizations detected a few isolated positive cells within some of the tentacles, suggesting that a cell migration occurs before the end of differentiation, whereas in *Hydra* nematocytes migrate only once differentiated. We propose two hypotheses to explain this difference. First, these cells may be microbasic-b-mastigophore nematoblasts that are carried into the tentacle with the general massive cell movement, together with the fully differentiated cells. Alternatively, these isolated undifferentiated cells and the differentiated nematocytes that continuously colonize the tentacle may represent two distinct cell populations corresponding to two nematocyte types. Supporting this hypothesis, the

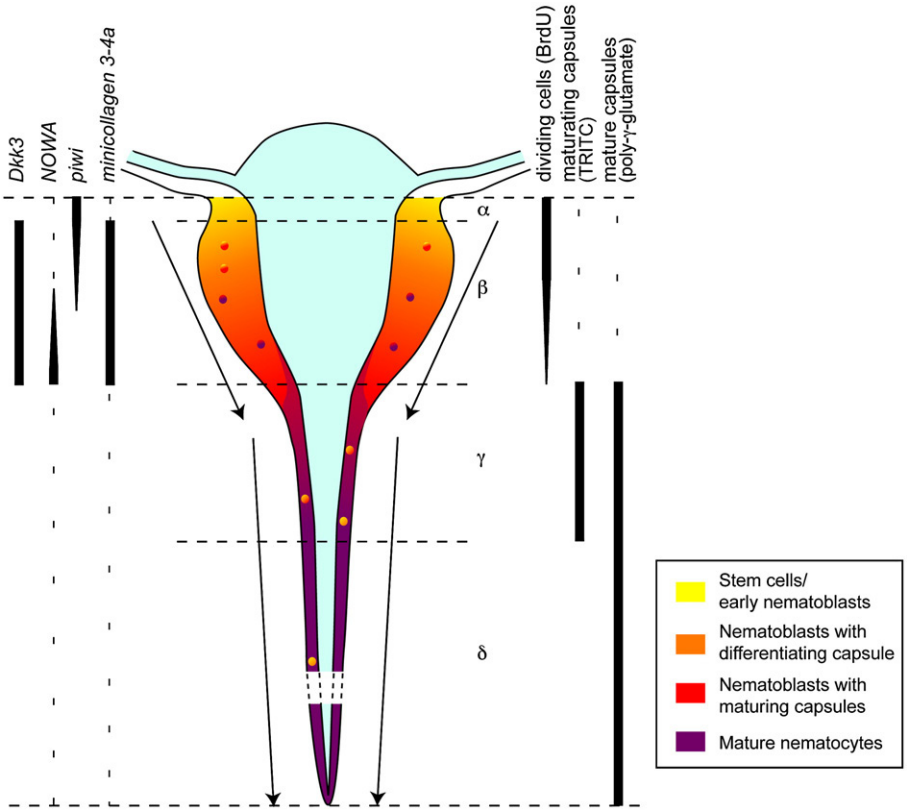

Fig. 7. General model of nematogenesis in the *Clytia* TBE. The nematogenesis stages are distributed in a proximo-distal succession. Gene expression patterns as well as cellular characteristics are shown. Dashes represent minority staining of scattered cells.

isolated cells were slightly bigger and rounder than other nematoblasts and could thus belong to the atrichous isorhiza category. Although in *Hydra* different nematoblasts populations cannot be distinguished by differential *minicollagen* mRNA expression (Kurz et al., 1991), differential migration pathways were described among nematocyte categories. Stenoteles start to migrate after a "lag-phase" not observed for atrichous isorhiza (Weber, 1995), which is reminiscent of what we observed in *Clytia*.

Advantages of the Clytia TBE as an experimental model for nematogenesis

The characteristics of nematogenesis in the tentacle bulb ectoderm of *Clytia* open unique experimental perspective for future studies of gene expression and regulation. In our model, the existence of a spatial progression of nematoblast stages along the bulb axis should greatly facilitate the identification of new genes involved in the various phases of nematogenesis (Fig. 7).

Because nematogenesis progresses from basis to tip of the bulb, the time frame in which a gene is expressed during the process is spatially integrated in the form of a crescent-shaped expression zone on the inner TBE. The lower and upper limits of this band along the bulb axis can in turn be taken as a rough indication about the time frame of the gene expression during nematogenesis (e.g. early, middle, late). Such property should be particularly helpful to develop systematic approaches, e.g. *in situ* screenings for identification of genes involved in the various phases of nematogenesis, or microarrays to compare transcriptomes at various levels of the TBE.

An additional useful property of the bulb is its capacity to survive and to regenerate tentacles and nematoblasts in culture following excision from the medusa in only sea water for several days (personal observation). This ability is likely to rely on the food digestion and storage capacity of the underlying endoderm (Bouillon, 1994). This feature would offer the opportunity to work on an individual, autonomous organ isolated from the influence of the rest of the organism and to restrict the effect of functional experiments to this area. Future attempts to investigate functional aspects of molecular regulation during nematogenesis could take advantage of the unique experimental opportunities offered by the tentacle bulb model. Indeed, the function of studied genes during nematogenesis could be tested and targeted by direct injection of dsRNA in the endodermal cavity or siRNA lipofection directly to the ectodermal surface.

Acknowledgments

We thank Pierrette Lamarre for technical help. We also specially thank Michel Vervoort for kindly providing the anti-phosphoH3 antibody; Aldine Amiel and Evelyn Houliston for the phalloidin staining; David Montero for help with SEM preparations and observation; Ghislaine Frébourg for Epon inclusion protocol; Claire Fayet for help with semi-thin and ultra-thin sections, coloration and TEM observation.

We would like to specially thank Evelyn Houliston for lab facilities, improving the English and, together with Eric Quéinnec, for their useful comments and critical reading of the manuscript. We also thank Muriel Jager and Roxane Chiori for fruitful discussions and advice on technical and theoretical aspects of our work. This work was supported by grants from the French Ministry of Research (ACI jeunes chercheurs), and a grant from the GIS "Institut de la Génomique Marine"—ANR blanche NT_NV_52. We thank the Consortium National de Recherche en Génomique and the Genoscope (Evry, France) for sequencing ESTs from *C. hemisphaerica*.

Appendix A. Supplementary data

Supplementary data associated with this article can be found, in the online version, at doi:10.1016/j.ydbio.2007.12.023.

References

Bode, H.R., 1988. Control of nematocyte differentiation in *Hydra*. In: Hessinger, D.A., Lenhoff, H.M. (Eds.), Biology of Nematocysts. Academic Press, Inc. Dan Diego, pp. 209–232.

Bode, H.R., 1996. The interstitial cell lineage of hydra: a stem cell system that arose early in evolution. J. Cell Sci. 109, 1155–1164.

Bode, H.R., David, C.N., 1978. Regulation of a multipotent stem cell, the interstitial cell of hydra. Prog. Biophys. Mol. Biol. 33, 189–206.

Boelsterli, U., 1977. An electron microscopic study of early developmental stages, myogenesis, oogenesis and cnidogenesis in the anthomedusa, *Podocoryne carnea* M. Sars. J. Morphol. 154, 259–289.

Bouillon, J., 1994. Classe des Hydrozoaires. In: Grassé, P.-P. (Ed), Traité de Zoologie, Cnidaires, Cténaires, 3(2), Masson, Paris, pp. 174, 202, 205, 206.

Brinkmann, M., Oliver, D., Thurm, U., 1996. Mechanoelectric transduction in nematocytes of a hydropolyp (Corynidae). J. Comp. Phys. 178, 125–138.

Brusca, R.C., Brusca, G.J., 2003. Invertebrates. Sinauer Associates, Sunderland.

Burnett, A.L., 1968. The acquisition, maintenance, and liability of the differentiated state in hydra. In: Hagens, H.-W. (Ed.), Results and Problems in Cell Differentiation. Springer-Verlag, Berlin, pp. 109–127.

Campbell, R.D., David, C.N., 1974. Cell cycle kinetics and development of *Hydra attenuata*. II. Interstitial cells. J. Cell Sci. 16, 349–358.

Chapman, D.M., 1974. Cnidarian histology. In: Muscatine, L., Lenhoff, H.M. (Eds.), Coelenterate Biology: Reviews and Perspectives. Academic Press, New York, pp. 1–92.

Chevalier, S., Martin, A., Leclère, L., Amiel, A., Houliston, E., 2006. Polarised expression of *FoxB* and *FoxQ2* genes during development of the hydrozoan *Clytia hemisphaerica*. Dev. Genes Evol. 216, 709–720.

Cikaluk, D.E., Tahbaz, N., Hendricks, L.C., DiMattia, G.E., Hansen, D., Pilgrim, D., Hobman, T.C., 1999. GERp95, a membrane-associated protein that belongs to a family of proteins involved in stem cell differentiation. Mol. Biol. Cell. 10, 3357–3372.

Collins, A.G., Schuchert, P., Marques, A.C., Jankowski, T., Medina, M., Schierwater, B., 2006. Medusozoan phylogeny and character evolution clarified by new large and small subunit rDNA data and an assessment of the utility of phylogenetic mixture models. Syst. Biol. 55, 97–115.

Cox, D.N., Chao, A., Baker, J., Chang, L., Qiao, D., Lin, H., 1998. A novel class of evolutionarily conserved genes defined by piwi are essential for stem cell self-renewal. Genes Dev. 12, 3715–3727.

David, C.N., Challoner, D., 1974. Distribution of interstitial cells and differentiating nematocytes in nests of *Hydra attenuata*. Am. Zool. 14, 537–542.

David, C.N., Gierer, A., 1974. Cell cycle kinetics and development. of *Hydra attenuata*. III. Nerve and nematocyte differentiation. J. Cell Sci. 16, 359–375.

David, C.N., Murphy, S., 1977. Characterization of interstitial stem cells in hydra by cloning. Dev. Biol. 58, 372–383.

Engel, U., Özbek, S., Streitwolf-Engel, R., Petri, B., Lottspeich, F., Holstein, T.W., 2002. Nowa, a novel protein with minicollagen Cys-rich domains, is involved in nematocyst formation in *Hydra*. J. Cell. Sci. 115, 3923–3934.

Fedders, H., Augustin, R., Bosch, T.C., 2004. A *Dickkopf-3*-related gene is expressed in differentiating nematocytes in the basal metazoan *Hydra*. Dev. Genes Evol. 214, 72–80.

Fetzer, C.P., 2002. A PIWI homolog is one of the proteins expressed exclusively during macronuclear development in the ciliate *Stylonychia lemnae*. Nucleic Acids Res. 30, 4380–4386.

Fujisawa, T., Nishimiya, C., Sugiyama, T., 1986. Nematocyte differentiation in hydra. Curr. Top. Dev. Biol. 20, 281–290.

Galliot, B., Schmid, V., 2002. Cnidarians as a model system for understanding evolution and regeneration. Int. J. Dev. Biol. 46, 39–48.

Gamse, J.T., Sive, H., 2001. Early anteroposterior division of the presumptive neurectoderm in *Xenopus*. Mech. Dev. 104, 21–36.

Gauchat, D., Escriva, H., Miljkovic-Licina, M., Chera, S., Langlois, M.C., Begue, A., Laudet, V., Galliot, B., 2004. The orphan COUP-TF nuclear receptors are markers for neurogenesis from cnidarians to vertebrates. Dev. Biol. 275, 104–123.

Grens, A., Mason, E., Marsh, J.L., Bode, H.R., 1995. Evolutionary conservation of a cell fate specification gene: the *Hydra* achaete-scute homolog has proneural activity in *Drosophila*. Development 121, 4027–4035.

Guindon, S., Gascuel, O., 2003. A simple, fast, and accurate algorithm to estimate large phylogenies by maximum likelihood. Syst. Biol. 52, 696–704.

Hansen, G.N., Williamson, M., Grimmelikhuijzen, C.J., 2000. Two-color double-labeling *in situ* hybridization of whole-mount *Hydra* using RNA probes for five different *Hydra* neuropeptide preprohormones: evidence for colocalization. Cell Tissue Res. 301, 245–253.

Hausmann, K., Holstein, T.W., 1985. Sensory receptor with bilateral symmetrical polarity. Naturwissenschaften 72, 145–146.

Hemmrich, G., Bosch, T.C.G., 2007. Compagen—a comparative genomics platform for basal Metazoa. Manuscript in preparation.

Holstein, T., 1981. The morphogenesis of nematocytes in *Hydra* and *Forskålia*: an ultrastructural study. J. Ultrastruct. Res. 75, 276–290.

Holstein, T., Tardent, P., 1984. An ultrahigh-speed analysis of exocytosis: nematocyst discharge. Science 223, 830–833.

Kass-Simon, G., Scappaticci, A.A., 2002. The behavioral and developmental physiology of nematocysts. Can. J. Zool. 80, 1772–1794.

Kurz, E.M., Holstein, T.W., Petri, B.M., Engel, J., David, C.N., 1991. Mini-collagens in hydra nematocytes. J. Cell. Biol. 115, 1159–1169.

Lentz, T.L., 1966. The Cell Biology of *Hydra*. North-Holland Publishing Co, Amsterdam.

Lin, H., Spradling, A.C., 1997. A novel group of pumilio mutations affects the asymmetric division of germline stem cells in the *Drosophila* ovary. Development 124, 2463–2476.

Lindgens, D., Holstein, T.W., Technau, U., 2004. Hyzic, the *Hydra* homolog of the *zic/odd-paired* gene, is involved in the early specification of the sensory nematocytes. Development 131, 191–201.

Lingel, A., Sattler, M., 2005. Novel modes of protein–RNA recognition in the RNAi pathway. Curr. Opin. Struct. Biol. 15, 107–115.

Mazet, F., Shimeld, S.M., 2002. The evolution of chordate neural segmentation. Dev. Biol. 251, 258–270.

Miljkovic-Licina, M., Gauchat, D., Galliot, B., 2004. Neuronal evolution: analysis of regulatory genes in a first-evolved nervous system, the hydra nervous system. Biosystems 76, 75–87.

Miljkovic-Licina, M., Chera, S., Ghila, L., Galliot, B., 2007. Head regeneration in wild-type hydra requires de novo neurogenesis. Development 134, 1191–1201.

Mochizuki, K., Fine, N.A., Fujisawa, T., Gorovsky, M.A., 2002. Analysis of a *piwi*-related gene implicates small RNAs in genome rearrangement in *Tetrahymena*. Cell 110, 689–699.

Momose, T., Houliston, E., 2007. Two oppositely localised *frizzled* RNAs as axis determinants in a cnidarian embryo. PLoS Biol. 4 (e70), 889–899.

Müller, P., Seipel, K., Yanze, N., Reber-Müller, S., Streitwolf-Engel, R., Stierwald, M., Spring, J., Schmid, V., 2003. Evolutionary aspects of developmentally regulated helix–loop–helix transcription factors in striated muscle of jellyfish. Dev. Biol. 255, 216–229.

Nüchter, T., Benoit, M., Engel, U., Özbek, S., Holstein, T.W., 2006. Nanosecond-scale kinetics of nematocyst discharge. Curr. Biol. 16, R316–R318.

Odenthal, J., Nusslein-Volhard, C., 1998. Fork head domain genes in zebrafish. Dev. Genes Evol. 208, 245–258.

Östman, C., 1979. Nematocysts of the Phialidium medusae of *Clytia hemisphaerica* (Hydrozoa, Campnulariidae) studied by light and electron microscopy. Zoon. 7, 125–142.

Qiao, D., Zeeman, A.M., Deng, W., Looijenga, L.H., Lin, H., 2002. Molecular characterization of *hiwi*, a human member of the *piwi* gene family whose overexpression is correlated to seminomas. Oncogene 21, 3988–3999.

Rebscher, N., Zelada-Gonzalez, F., Banisch, T.U., Raible, F., Arendt, D., 2007. *Vasa* unveils a common origin of germ cells and of somatic stem cells from the posterior growth zone in the polychaete *Platynereis dumerilii*. Dev. Biol. 306, 599–611.

Reddien, P.W., Oviedo, N.J., Jennings, J.R., Jenkin, J.C., Sanchez Alvarado, A., 2005. SMEDWI-2 is a PIWI-like protein that regulates planarian stem cells. Science 310, 1327–1330.

Rossi, L., Salvetti, A., Lena, A., Batistoni, R., Deri, P., Pugliesi, C., Loreti, E., Gremigni, V., 2006. *DjPiwi-1*, a member of the *PAZ-Piwi* gene family, defines a subpopulation of planarian stem cells. Dev. Genes Evol. 216, 335–346.

Seipel, K., Yanze, N., Schmid, V., 2004. The germ line and somatic stem cell gene *Cniwi* in the jellyfish *Podocoryne carnea*. Int. J. Dev. Biol. 48, 1–7.

Slautterback, D.B., Fawcett, D.W., 1959. The development of the cnidoblasts of hydra. J. Biophys. Biochem. Cytol. 5, 441–452.

Spring, J., Yanze, N., Middel, A.M., Stierwald, M., Groger, H., Schmid, V., 2000. The mesoderm specification factor twist in the life cycle of jellyfish. Dev. Biol. 228, 363–375.

Szczepanek, S., Cikala, M., David, C.N., 2002. Poly-gamma-glutamate synthesis during formation of nematocyst capsules in *Hydra*. J. Cell Sci. 115, 745–751.

Tan, C.H., Lee, T.C., Weeraratne, S.D., Korzh, V., Lim, T.M., Gong, Z., 2002. *Ziwi*, the zebrafish homologue of the *Drosophila piwi*: co-localization with vasa at the embryonic genital ridge and gonad-specific expression in the adults. Mech. Dev. 119 (Suppl 1), S221–S224.

Teo, R., Möhrlen, F., Plickert, G., Müller, W.A., Frank, U., 2006. An evolutionary conserved role of Wnt signaling in stem cell fate decision. Dev. Biol. 289, 91–99.

Thurm, U., Brinkmann, M., Golz, R., Holtmann, M., Oliver, D., Sieger, T., 2004. Mechanoreception and synaptic transmission of hydrozoan nematocytes. Hydrobiologia 530–531, 97–105.

Weber, J., 1995. Novel tools for the study of development, migration and turnover of nematocytes (cnidarian stinging cells). J. Cell. Sci. 108, 403–412.

Westfall, J.A., 1966. The differentiation of nematocytes and associated structures in Cnidaria. Cell Tissue Res. 75, 381–403.

Westfall, J.A., 1996. Ultrastructure of synapses in the first-evolved nervous systems. J. Neurocytol. 25, 735–746.

Whelan, S., Goldman, N., 2001. A general empirical model of protein evolution derived from multiple protein families using a maximum-likelihood approach. Mol. Biol. Evol. 18, 691–699.